Taxonomy of Centaurs and Trans-Neptunian Objects

Maria Antonietta Barucci, Irina Belskaya, Marcello Fulchignoni, Mirel Birlan

The Astronomical Journal, 130:1291–1298, 2005 September

TAXONOMY OF CENTAURS AND TRANS-NEPTUNIAN OBJECTS

M. A. Barucci,[1] I. N. Belskaya,[2] M. Fulchignoni,[1,3] and M. Birlan[4]
Received 2005 February 18; accepted 2005 May 13

ABSTRACT

Trans-Neptunian objects (TNOs) and Centaurs display the widest color diversity in comparison to other small solar system bodies. The investigation of their properties can help in understanding the evolution of these objects. In this paper we propose a classification scheme based on multivariate statistical analysis of a homogeneous, high-quality set of $B-V$, $V-R$, $V-I$, and $V-J$ color indices. Analyzing a sample of 51 objects and using a high confidence level, four groups have been identified and named: *BB*, *BR*, *IR*, and *RR*. The group *BB* contains objects with neutral color and *RR* those with very red color, while the others have intermediate behavior. We extend the analysis to 84 other objects for which three colors are available, obtaining a preliminary classification. A tentative interpretation of these groups in terms of surface characteristics is given.

Key words: Kuiper Belt — methods: statistical — techniques: photometric

1. INTRODUCTION

Trans-Neptunian objects (TNOs) or the so-called Edgeworth–Kuiper Belt objects are believed to represent the most pristine and thermally unprocessed objects in the solar system that are accessible to ground-based observations. They are presumed to be remnants of external planetesimal swarms. Since the first discovery in 1992, more than 1000 objects have been detected, and their number increases continuously. These objects can be divided dynamically into several classes: classical objects, with orbits having low eccentricities and inclinations (semimajor axes between about 42 and 48 AU); resonant objects, which are trapped in resonances with Neptune with the majority in or near the 3:2 mean motion resonance; scattered objects, with high-eccentricity, high-inclination orbits and a perihelion distance near $q = 35$ AU; and extended scattered disk objects, which do not have gravitational interactions with Neptune. With this population we can also associate the Centaurs, which seem to come from TNOs and were injected into their present orbits by gravitational instabilities and collisions.

The study of physical properties of TNOs and Centaurs can provide essential information about the conditions present in the early solar system environment. The physical and chemical knowledge of these objects is still very limited (see Barucci et al. 2004 for a review), with little information available on the compositional properties of their surfaces. Spectroscopy is the best method to investigate the surface composition of these remote objects. However, given their faintness, visible and near-infrared spectra are available only for a few of them at best, with very low signal-to-noise ratio. Today, photometry is the only technique that provides data for a large number of objects, particularly in the visible region. Recent large programs (Doressoundiram et al. 2001, 2002, 2005b; Boehnhardt et al. 2002; Peixinho et al. 2004) have provided high-quality, homogeneous *B*, *V*, *R*, and *I* colors for about 130 objects. The relevant statistical analyses have been performed, and all possible correlations between optical colors and orbital parameters have been analyzed (see Doressoundiram 2003 for a review). Tegler & Romanishin (1998, 2000, 2003), with a statistic based on the analysis of only two colors, $B-V$ and $V-R$, found a division into two distinct populations: one consisting of objects whose surface colors were similar to those of the Sun and the other consisting of the reddest objects known in the solar system.

The investigation of color diversity is important and can be a diagnostic of possible composition diversity and/or the different evolutions from different physical processes affecting the surfaces of objects. When dealing with a large number of objects, it is important to distinguish groups of objects with similar surface properties. Such an approach to studying the physical properties of asteroids has resulted in a taxonomy scheme based mostly on surface colors and albedos and has become an efficient tool in asteroid investigations.

In this paper we apply to 51 TNOs and Centaurs the same techniques used to classify asteroids in the 1980s. The first attempts at such an analysis were devoted to groups of 22 objects (Barucci et al. 2001) and 34 objects (Fulchignoni et al. 2003) and showed that $V-I$ and $V-J$ colors are the key parameters in dividing a sample into homogeneous groups. Barucci et al. (2001) found a continuous spread of these objects between neutral to very red colors. Further analysis yielded four groups, while Fulchignoni et al. (2003) showed that the larger the sample, the finer its description could be.

In this paper we analyze photometric data of a sample of 51 objects for which highly homogeneous four-color indices ($B-V$, $V-R$, $V-I$, and $V-J$) exist, and then we enlarge the statistics to a large sample of 135 objects for which only three-color indices ($B-V$, $V-R$, and $V-I$) are available.

2. OBSERVATIONAL DATA

We considered all the available colors published after 1996 for TNOs and Centaurs. We obtained (1) a set of data for 135 objects observed in the *B*, *V*, *R*, and *I* bands, (2) a set of 51 objects observed in the *B*, *V*, *R*, *I*, and *J* bands with high-quality homogeneous data, and (3) a subsample of 37 objects also including the *H* band. We selected as the primary sample the complete set of 51 objects observed in five filters (*B*, *V*, *R*, *I*, and *J*), owing to the importance of $V-J$ colors as shown by a previous analysis (Barucci et al. 2001). The list of objects and their colors together with the references to the original data are given in Table 1. When multiple observations of an object were available, we

[1] LESIA, Observatoire de Paris, 92195 Meudon Principal Cedex, France; antonella.barucci@obspm.fr.
[2] Institute of Astronomy, Kharkiv National University, 61022 Kharkiv, Ukraine.
[3] Université Denis Diderot—Paris 7, 2 Place Jussieu, 75005 Paris, France.
[4] IMCCE, Observatoire de Paris, 77 Avenue Denfert-Rochereau, 75014 Paris, France.

TABLE 1

Average Colors of the Selected Sample of 51 Objects and the Proposed Taxonomical Classification

Object	Type[a]	$B-V$	$V-R$	$V-I$	$V-J$	$V-H$	References	Group
Sun	...	0.67	0.36	0.69	1.08	1.37	1, 2	
2060 Chiron	C	0.66 ± 0.04	0.36 ± 0.01	0.74 ± 0.04	1.13 ± 0.06	1.42 ± 0.07	14, 15, 17, 25	*BB*
5145 Pholus	C	1.23 ± 0.03	0.77 ± 0.01	1.57 ± 0.01	2.59 ± 0.01	2.97 ± 0.01	8, 15, 17, 25	*RR*
7066 Nessus	C	1.09 ± 0.01	0.79 ± 0.01	1.47 ± 0.03	2.29 ± 0.01	2.57 ± 0.10	14, 15, 17, 25	*RR*
8405 Asbolus	C	0.75 ± 0.01	0.47 ± 0.02	0.98 ± 0.01	1.65 ± 0.01	2.02 ± 0.06	15, 17, 18, 19, 25	*BR*
10199 Chariklo	C	0.80 ± 0.02	0.48 ± 0.01	1.01 ± 0.01	1.74 ± 0.02	2.15 ± 0.01	3, 5, 17, 25, 42	*BR*
10370 Hylonome	C	0.69 ± 0.06	0.43 ± 0.02	0.96 ± 0.03	1.32 ± 0.01	1.50 ± 0.08	5, 9, 15, 17, 25, 42	*BR*
15788 1993 SB	R	0.80 ± 0.02	0.47 ± 0.01	1.01 ± 0.01	1.43 ± 0.11		3, 4, 6, 20, 22	*BR*
15789 1993 SC	R	1.08 ± 0.08	0.70 ± 0.06	1.49 ± 0.04	2.42 ± 0.11	2.82 ± 0.20	3, 4, 7, 8, 14,	*RR*
15820 1994 TB	R	1.10 ± 0.02	0.68 ± 0.02	1.42 ± 0.04	2.35 ± 0.12	2.76 ± 0.08	3, 4, 8, 9, 11, 12, 20	*RR*
15874 1996 TL_{66}	S	0.72 ± 0.03	0.36 ± 0.01	0.73 ± 0.01	1.28 ± 0.08	1.63 ± 0.14	3, 4, 5, 7, 10	*BB*
15875 1996 TP_{66}	R	1.05 ± 0.06	0.66 ± 0.02	1.31 ± 0.07	2.16 ± 0.04	2.33 ± 0.06	3, 4, 5, 7, 9, 10	*RR*
19299 1996 SZ_4	R	0.75 ± 0.08	0.52 ± 0.03	0.97 ± 0.14	1.87 ± 0.13		3, 4, 22, 24	*BR*
19308 1996 TO_{66}	Cl	0.67 ± 0.03	0.40 ± 0.02	0.74 ± 0.02	0.85 ± 0.10	0.64 ± 0.17	3, 5, 7, 10, 16, 26, 27	*BB*
19521 Chaos	Cl	0.93 ± 0.03	0.62 ± 0.01	1.16 ± 0.05	1.88 ± 0.05	2.28 ± 0.05	4, 9, 10, 11, 12, 22	*IR*
20000 Varuna	Cl	0.88 ± 0.03	0.61 ± 0.02	1.25 ± 0.02	2.01 ± 0.05		4, 9, 13, 28	*IR*
24835 1995 SM_{55}	Cl	0.65 ± 0.01	0.38 ± 0.02	0.71 ± 0.02	1.01 ± 0.01	0.54 ± 0.07	4, 6, 9, 10, 11, 12, 28	*BB*
24952 1997 QJ_4	R	0.76 ± 0.04	0.43 ± 0.06	0.81 ± 0.05	1.23 ± 0.31		3, 4, 6, 20, 24	*BB*
26181 1996 GQ_{21}	S	1.01 ± 0.07	0.71 ± 0.02	1.42 ± 0.06	2.44 ± 0.06	2.92 ± 0.07	11, 13, 24, 29	*RR*
26308 1998 SM_{165}	Cl	0.97 ± 0.03	0.69 ± 0.04	1.29 ± 0.07	2.37 ± 0.01	2.88 ± 0.08	4, 11, 12, 22	*RR*
26375 1999 DE_9	S	0.97 ± 0.03	0.58 ± 0.01	1.15 ± 0.01	1.89 ± 0.07	2.19 ± 0.01	3, 9, 11, 20, 29, 30	*IR*
29981 1999 TD_{10}	S	0.77 ± 0.02	0.48 ± 0.02	0.98 ± 0.03	1.81 ± 0.06		4, 20, 28	*BR*
32532 Thereus	C	0.75 ± 0.05	0.49 ± 0.02	0.93 ± 0.01	1.66 ± 0.03	2.17 ± 0.06	17, 31, 32	*BR*
32929 1995 QY_9	R	0.70 ± 0.02	0.51 ± 0.04	0.86 ± 0.06	2.02 ± 0.01		4, 6, 9, 14	*BR*
33128 1998 BU_{48}	C	0.95 ± 0.08	0.64 ± 0.02	1.18 ± 0.01	2.27 ± 0.05	2.76 ± 0.09	9, 11, 12, 13, 17	*RR*
33340 1998 VG_{44}	R	0.91 ± 0.01	0.60 ± 0.01	1.23 ± 0.11	1.80 ± 0.16	2.23 ± 0.06	4, 9, 10	*IR*
35671 1998 SN_{165}	Cl	0.71 ± 0.06	0.42 ± 0.03	0.82 ± 0.01	1.27 ± 0.05		3, 4, 6, 9, 20	*BB*
38628 Huya	R	0.95 ± 0.02	0.59 ± 0.02	1.21 ± 0.02	1.97 ± 0.05		3, 4, 9, 24, 28, 33, 34	*IR*
40314 1999 KR_{16}	Cl	1.06 ± 0.03	0.76 ± 0.01	1.50 ± 0.03	2.37 ± 0.10	2.95 ± 0.06	3, 11, 12, 13, 35, 36	*RR*
44594 1999 OX_3	C	1.14 ± 0.02	0.68 ± 0.02	1.38 ± 0.03	2.11 ± 0.08	2.59 ± 0.07	4, 9, 11, 17, 22, 35, 43	*RR*
47171 1999 TC_{36}	R	1.01 ± 0.04	0.69 ± 0.03	1.32 ± 0.05	2.33 ± 0.07	2.74 ± 0.03	4, 9, 10, 11, 12, 30, 41	*RR*
47932 2000 GN_{171}	R	0.92 ± 0.01	0.63 ± 0.01	1.21 ± 0.02	1.77 ± 0.06		4, 13, 24	*IR*
48639 1995 TL_8	S	1.04 ± 0.01	0.69 ± 0.01	1.33 ± 0.01	2.42 ± 0.05	2.82 ± 0.07	11, 20	*RR*
52975 Cyllarus	C	1.12 ± 0.04	0.69 ± 0.01	1.36 ± 0.03	2.42 ± 0.07	2.87 ± 0.09	9, 10, 11, 12, 17	*RR*
54598 Bienor	C	0.68 ± 0.02	0.44 ± 0.03	0.87 ± 0.03	1.69 ± 0.06	2.12 ± 0.17	9, 11, 12, 17, 30, 41	*BR*
55565 2002 AW_{197}	Cl	0.90 ± 0.03	0.62 ± 0.03	1.18 ± 0.03	1.82 ± 0.06	2.15 ± 0.06	39	*IR*
55576 2002 GB_{10}	C	1.12 ± 0.03	0.72 ± 0.03	1.32 ± 0.03	2.11 ± 0.08	2.40 ± 0.08	39	*RR*
58534 1997 CQ_{29}	Cl	0.99 ± 0.01	0.73 ± 0.06	1.29 ± 0.03	1.84 ± 0.37		3, 6, 9, 10, 16	*RR*
60558 2000 EC_{98}	S	0.85 ± 0.08	0.47 ± 0.01	0.94 ± 0.02	1.49 ± 0.10	2.05 ± 0.06	11, 12, 17, 24	*BR*
63252 2001 BL_{41}	C	0.72 ± 0.05	0.48 ± 0.03	1.06 ± 0.03	1.65 ± 0.07	2.02 ± 0.05	17, 29, 30, 35	*BR*
79360 1997 CS_{29}	Cl	1.08 ± 0.03	0.66 ± 0.04	1.25 ± 0.03	2.06 ± 0.03	2.45 ± 0.08	3, 4, 5, 9, 10, 11	*RR*
83982 2002 GO_9	C	1.13 ± 0.03	0.76 ± 0.03	1.44 ± 0.03	2.44 ± 0.06	2.81 ± 0.06	39	*RR*
90377 Sedna	ES	1.08 ± 0.06	0.67 ± 0.08	1.26 ± 0.07	2.06 ± 0.03	2.61 ± 0.06	21	*RR*
90482 Orcus	R	0.68 ± 0.04	0.37 ± 0.04	0.74 ± 0.04	1.08 ± 0.04	1.21 ± 0.05	40	*BB*
91133 1998 HK_{151}	R	0.72 ± 0.05	0.49 ± 0.03	0.88 ± 0.01	1.57 ± 0.09		4, 9, 10	*BR*
1996 TQ_{66}	R	1.19 ± 0.02	0.66 ± 0.03	1.44 ± 0.14	2.41 ± 0.08		3, 4, 5, 6	*RR*
1996 TS_{66}	Cl	1.06 ± 0.03	0.72 ± 0.03	1.31 ± 0.08	1.87 ± 0.03		3, 5, 7, 16	*RR*
1998 WU_{24}	?	0.78 ± 0.03	0.53 ± 0.04	0.99 ± 0.03	1.67 ± 0.04		38	*BR*
1999 CD_{158}	Cl	0.86 ± 0.01	0.52 ± 0.02	1.10 ± 0.04	1.86 ± 0.07	2.30 ± 0.09	9, 11, 12	*BR*
2000 OJ_{67}	Cl	1.05 ± 0.06	0.67 ± 0.05	1.27 ± 0.07	1.98 ± 0.10	2.26 ± 0.08	9, 11	*RR*
2000 OK_{67}	Cl	0.82 ± 0.06	0.60 ± 0.05	1.22 ± 0.08	2.42 ± 0.08	2.88 ± 0.08	9, 11, 12	...
2000 PE_{30}	S	0.71 ± 0.05	0.38 ± 0.04	0.83 ± 0.04	1.40 ± 0.10	1.82 ± 0.09	9, 11, 12	*BB*

[a] (C) centaurs; (Cl) classical; (R) resonant; (S) scattered; (ES) extended scattering disk; (?) unusual, Halley family comet orbit.

References.—(1) Hardorp 1980; (2) Hartmann et al. 1982; (3) Jewitt & Luu 2001; (4) McBride et al. 2003; (5) Tegler & Romanishin 1998; (6) Gil-Hutton & Licandro J. 2001; (7) Jewitt & Luu 1998; (8) Tegler & Romanishin 1997; (9) Doressoundiram et al. 2002; (10) Boehnhardt et al. 2001; (11) Delsanti et al. 2005; (12) Delsanti et al. 2004; (13) Sheppard & Jewitt 2002; (14) Luu & Jewitt 1996; (15) Davies et al. 1998; (16) Davies et al. 2000; (17) Bauer et al. 2003; (18) Romanishin et al. 1997; (19) Romon-Martin et al. 2002; (20) Delsanti et al. 2001; (21) Barucci et al. 2005; (22) Tegler & Romanishin 2000; (23) Davies et al. 1997; (24) Boehnhardt et al. 2002; (25) Davies 2000; (26) Hainaut et al. 2000; (27) Barucci et al. 1999; (28) Tegler & Romanishin 2003; (29) Doressoundiram et al. 2003; (30) Tegler et al. 2003; (31) Barucci et al. 2002; (32) Farnham & Davies 2003; (33) Ferrin et al. 2001; (34) Schaefer & Rabinowitz 2002; (35) Peixinho et al. 2003; (36) Trujillo & Brown 2002; (37) Doressoundiram et al. 2001; (38) Davies et al. 2001; (39) Doressoundiram et al. 2005a; (40) de Bergh et al. 2005; (41) Dotto et al. 2003a; (42) McBride et al. 1999; (43) Doressoundiram et al. 2005b.

TABLE 2
EIGENVECTORS, EIGENVALUES, AND PERCENTAGE OF TOTAL VARIANCE CONTRIBUTED BY EACH EIGENVALUE FROM THE PC ANALYSIS

Variable	1	2	3	4
$B-V$	0.290	0.577	−0.755	−0.114
$V-R$	0.225	0.278	0.160	0.920
$V-I$	0.436	0.526	0.626	−0.375
$V-J$	0.821	−0.560	−0.110	−0.013
Eigenvalues	0.282	0.014	0.002	0.001
Percentage of total variance	94.195	4.721	0.767	0.316

adopted the mean values of their colors weighted with the inverse of the error of individual measurement and used the standard deviation as the associated error. In the case of a single measurement we selected only those objects for which colors were determined with an error less than 0.1 mag. The selected data represent a homogeneous data set in the *B*, *V*, *R*, *I*, and *J* bands obtained by the same observer during the same run or intercalibrated through *V* measurements.

3. STATISTICAL ANALYSIS

We applied to the 51 TNOs and Centaurs (the sample) described by the four-color indices $B-V$, $V-R$, $V-I$, and $V-J$ (the variables) the same statistical analysis used in the 1980s to classify the asteroid population: the *G*-mode analysis from Barucci et al. (1987) and principal component analysis (Tholen 1984; Tholen & Barucci 1989). Principal components are linear combinations of the original variables, where the coefficients represent the relative importance of a variable within a principal component. These coefficients are the eigenvectors of the variance-covariance matrix of the variables. The sum of the eigenvalues of this matrix (its trace) accounts for the total variance of the sample. Each eigenvalue reflects the percentage contributed by each principal component to the total variance.

The results of this analysis (reported in Table 2) show that the first principal component (PC1) accounts for most of the variance of the sample (94%), with 46% due to $V-J$; PC2 adds less than 5% to the total variance. Most of the information is concentrated in PC1, which shows a continuous trend from the objects having a neutral color with respect to the Sun (lower PC1 scores) toward being the reddest objects of the solar system (higher PC1 scores). The object number density along the PC1 is not homogeneous, indicating the presence of some grouping that overlaps the continuous trend. In Figure 1 the histogram represents the number of objects projected onto the PC1, showing four peaks. The relationship between the variables used is probably nonlinear, so the PC analysis does not allow us to discriminate between the intrinsic structures of these groups within only one component.

For this reason we use a powerful statistical grouping method to recognize the structure of the number density distribution on the PC1 axis. The *G*-mode method (Coradini et al. 1977) allows the user to obtain an automatic clustering of a statistical sample containing *N* objects described by *M* variables (for a total of $M \times N$ degrees of freedom [dof]; the dof must be >100) in terms of homogeneous taxonomic groups with no a priori grouping criteria and taking into account the instrumental errors in measuring each variable. The method also gives indications as to the relative importance of the variables in separating the groups.

The original multivariate sample is collapsed into a univariate sample through successive transformations. The new variable (g) is normalized to a quasi-Gaussian distribution with a mean equal to 0 and a variance equal to 1; N' out of the *N* elements are

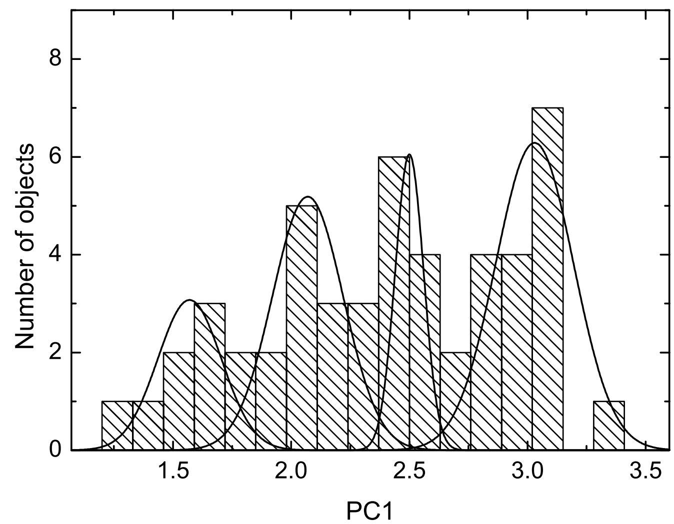

FIG. 1.—Number of objects projected onto the PC1 axis (*histogram*). The four Gaussian curves, computed using the average values of the four groups and the standard deviations obtained by the *G*-mode analysis, have been transformed into PC space and superposed on the histogram.

selected on the basis of a test of the hypothesis of membership in the first group, which comes out through an automatic choice once a starter is selected. The starter is defined as the set of the three elements having the minimum reciprocal distance. The selection procedure is iterated using as starter all the selected elements until their number N' does not change. The method is then iterated on the $N-N'$ elements left, in order to identify the second group, composed of N'' elements. The iteration proceeds on $N-(N'+N'')$ elements, and so on, until all the elements are classified into homogeneous groups. Homogeneous means that each group belongs to the same statistical population characterized by mean values of variables and relative standard deviations. The membership of an element in a given group, or the selection criteria, is based on the statistical inference rules, the only a priori choice in the decision process being that of the confidence level defined as the probability of accepting the tested hypothesis. The user selects the confidence level that corresponds to a given critical value *Q*.

Using the *G*-mode analysis, we analyzed a sample of 51 objects, and $B-V$, $V-R$, $V-I$, and $V-J$ colors were taken as variables ($51 \times 4 = 204$ dof). This data set is listed in Table 1. Four homogeneous groups were obtained using a high confidence level *Q* (corresponding to 3 σ). The weight of each variable in separating these groups was 32% for the $V-I$ color, 26% for $V-R$, 22% for $V-J$, and 20% for $B-V$, implying that all variables contribute to the definition of the four groups. In Table 3 the number of samples, the color average value, and the relative standard deviation for each group are given.

To verify the consistence of these groups with the indication obtained by the PC analysis, we use the values of Table 3, transformed into PC space, to superpose the distributions representing the four groups found by the *G*-mode analysis on the histogram in Figure 1. Each Gaussian, representing the relative group, is centered on the average value of PC1, has the same standard deviation, and has an area representing the number of objects belonging to its group. The χ^2 test shows that the distribution represented by the histogram in Figure 1 and that corresponding to the sum of the four Gaussians representing the groups are similar within the 95% probability level. This implies that the four groups are at the origin of the nonhomogeneity of the PC1 number density.

TABLE 3
The Relative Number of Samples, Average Color, and Relative Standard Deviation for the Four Taxonomic Groups Attained by the *G*-Mode Analysis in the Sample of 51 Objects

Class	Number of Objects	$B-V$	$V-R$	$V-I$	$V-J$
BB	8	0.70 ± 0.04	0.39 ± 0.03	0.77 ± 0.05	1.16 ± 1.17
BR	14	0.76 ± 0.06	0.49 ± 0.03	0.9 ± 0.07	1.67 ± 0.19
IR	7	0.92 ± 0.03	0.61 ± 0.03	1.20 ± 0.04	1.88 ± 0.09
RR	21	1.08 ± 0.08	0.71 ± 0.04	1.37 ± 0.09	2.27 ± 0.20

The distributions of the objects within the four groups are illustrated in Figure 2. The two complementary three-dimensional plots, namely, the ($B-V$, $V-R$, $V-I$) and ($B-V$, $V-R$, $V-J$) color spaces, show the different behaviors of the four groups, as well as the role of each color (particularly $V-I$ and $V-J$) in assigning the samples to each group. One object, 2000 OK_{67}, does not belong to any group.

Moreover, we analyzed a subset of 37 objects for which the $V-H$ color was also available. *G*-mode analysis applied to this subsample described by five colors (for a total of $37 \times 5 = 185$ dof) provides practically the same well-determined four groups. The same objects fall in the same groups that were obtained with four variables. The color average $V-H$ and the relative standard deviation for each group are 1.21 ± 0.52 (*BB*), 2.04 ± 0.24 (*BR*), 2.21 ± 0.06 (*IR*), and 2.70 ± 0.24 (*RR*).

On the basis of these results, we propose to introduce a taxonomy of TNOs and Centaurs based on their surface broadband colors. A two-letter designation for the derived groups is introduced to distinguish TNO taxonomy from the asteroid one. Objects having a neutral color with respect to the Sun are classified as the *BB* ("blue") group, and those having a very high red color are classified as *RR* ("red"). The *BR* group consists of objects with an intermediate blue-red color, while the *IR* group includes moderately red objects. 2000 OK_{67}, which the *G*-mode analysis left out of this scheme, might be considered as a "single-object group" in a manner similar to 4 Vesta, 1862 Apollo, and 349 Dembowska, which formed the V, Q, and R classes, respectively, in the Tholen asteroid taxonomy (Tholen & Barucci 1989). Since then, the V class has been populated by plenty of small asteroids (Binzel & Xu 1993), and several new objects can be considered to belong to the Q and R classes (Bus & Binzel 2002). The assignment of each object to one of these groups is reported in the last column of Table 1.

The *G*-mode analysis has been extended (Fulchignoni et al. 2000) to assign to one of the already defined taxonomic groups any object for which the same set of variables becomes available. Moreover, even if a subset of the variables used in the initial development of the taxonomy is known for an object, the algorithm allows us to assign a preliminary indication of its likely group. The lack of information on a variable is reflected by the fact that an object could be assigned to two different classes when that variable is the one that discriminates between these classes.

We applied this algorithm to each of the 84 other TNOs for which the $B-V$, $V-R$, and $V-I$ colors are available. In Table 4 we report a preliminary classification for these objects, but their belonging to a given group always has to be considered with some caution because it is only an indication obtained with an incomplete data set. As an example, consider the object 2000 OK_{67}; when one applies the algorithm using four variables it cannot be assigned to any class, confirming the result obtained directly by the *G*-mode analysis, but if one does not take into consideration its $V-J$ color, the algorithm assigns it to the *IR* group because of its similitude in ($B-V$, $V-R$, $V-I$) space to the average value of that group. A double assignment is obtained for 13 objects, while 15 objects are not classified at all. If the single-object group is added to the four main groups, all the objects that were classified on the basis of the four classes continue to be assigned to the same groups, and three of the nonclassified objects (20% of the total) are attributed to the fifth group. This consideration

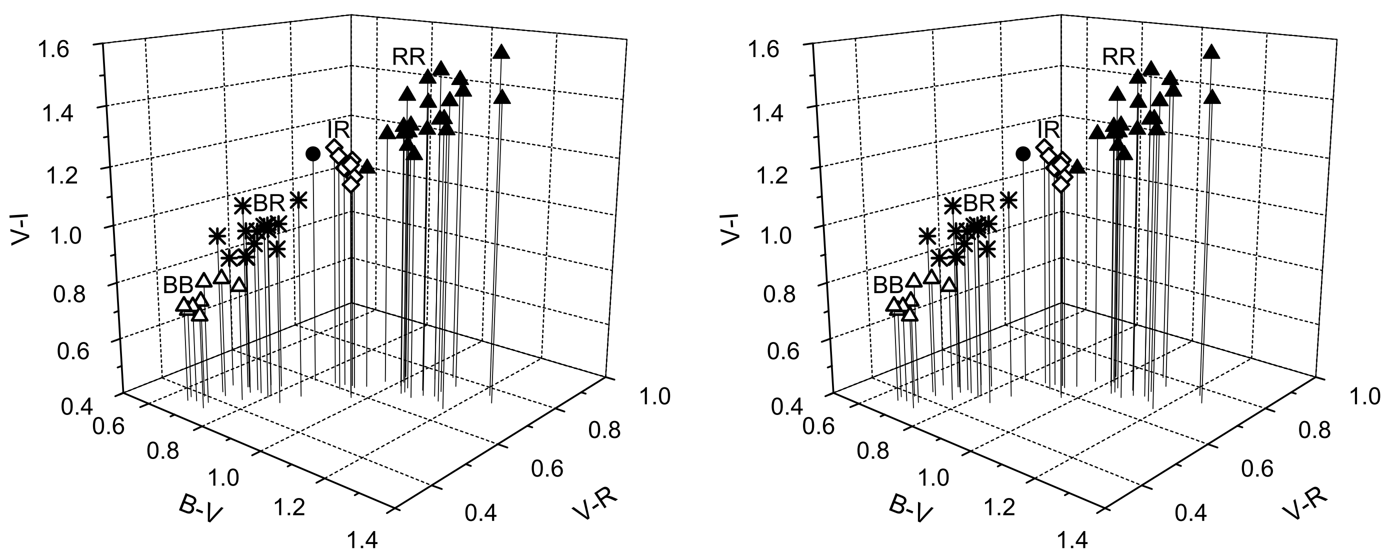

Fig. 2.—Well-separated groups in two complementary three-dimensional spaces, namely, ($B-V$, $V-R$, and $V-I$) (*left*) and ($B-V$, $V-R$, and $V-J$) (*right*). The object 2000 OK_{67} (*circle*) does not belong to any group.

TABLE 4

Preliminary Classification for the 84 Other Objects Based on Three-Color Indices ($B - V$, $V - R$, and $V - I$)

Object	*G*-Mode Class	Object	*G*-Mode Class
15760 1992 QB_1	*RR*	1996 RR_{20}	*RR*
15810 1994 JR_1	...	1996 TK_{66}	*RR*
15836 1995 DA_2	...	1997 QH_4	*RR*
15883 1997 CR_{29}	*BR*	1997 RT_5	...
16684 1994 JQ_1	*RR*	1998 KG_{62}	*IR-RR*
19255 1994 VK_8	*RR*	1998 UR_{43}	*BR*
28978 Ixion	*IR-RR*	1998 WS_{31}	*BR*
31824 Elatus	*RR-IR*	1998 WT_{31}	*BB*
33001 1997 CU_{29}	*RR*	1998 WV_{31}	*BR*
38083 Rhadamanthus	*BR*	1998 WZ_{31}	*BB-BR*
38084 1999 HB12	*BR*	1998 XY_{95}	*RR*
42301 2001 UR_{163}	...	1999 CB_{119}	*RR*
49036 Pelion	*BR*	1999 CF_{119}	*BR*
52872 Okyrnoe	*BR*	1999 CX_{131}	*RR*
55636 2002 TX_{300}	*BB*	1999 HC_{12}	*BR*
59358 1999 CL_{158}	*BB-BR*	1999 HR_{11}	...
60454 2000 CH_{105}	*RR*	1999 HS_{11}	*RR*
60608 2000 EE_{173}	*IR*	1999 OE_4	*RR*
60620 2000 FD_8	*RR*	1999 OJ_4	*RR*
60621 2000 FE_8	*BR*	1999 OM_4	*RR*
66452 1999 OF_4	*RR*	1999 RB_{216}	*BR*
69986 1998 WW_{24}	*BR*	1999 RE_{215}	*RR*
69988 1998 WA_{31}	*BR*	1999 RX_{214}	*RR-IR*
69990 1998 WU_{31}	...	1999 RY_{214}	*BR*
79978 1999 CC_{158}	*IR-RR*	1999 XX_{143}	*RR*
79983 1999 DF_9	*RR*	2000 CL_{104}	*RR*
82075 2000 YW_{134}	*BR*	2000 FZ_{53}	...
82158 2001 FP_{185}	...	2000 GP_{183}	*BB-BR*
85633 1998 KR_{65}	*RR*	2001 CZ_{31}	*BR*
86047 1999 OY_3	*BB*	2001 KA_{77}	*RR*
86177 1999 RY_{215}	*BR*	2001 KD_{77}	*RR*
91205 1998 US_{43}	*BR*	2001 KP_{77}	...
91554 1999 RZ_{215}	...	2001 KY_{76}	...
95626 2002 GZ_{32}	*BR*	2001 QF_{298}	*BB*
1993 RO	*IR-RR*	2001 QY_{297}	*BR*
1993 FW	*RR-IR*	2001 UQ_{18}	*RR*
1994 ES_2	...	2002 DH_5	*BR-BB*
1994 EV_3	*RR*	2002 GF_{32}	*RR*
1994 TA	*RR*	2002 GH_{32}	...
1995 HM_5	*BR*	2002 GJ_{32}	...
1995 WY_2	*RR-IR*	2002 GP_{32}	...
1996 RQ_{20}	*IR-RR*	2002 GV_{32}	*RR*

suggests that other groups could be found and that the taxonomy can still be enlarged and refined.

The average values of the five broadband colors obtained for each group and the relative error bars are represented in Figure 3 as reflectances $R_{c\lambda}$ normalized to the Sun and to the V colors:

$$R_{c_\lambda} = 10^{\pm 0.4(c_\lambda - c_{\lambda 0})},$$

where c_λ and $c_{\lambda 0}$ are the $\lambda - V$ colors of the object and of the Sun, respectively.

4. DISCUSSION

The four groups found by *G*-mode analysis are well defined and homogeneous in color properties. The investigation of TNOs by analyzing the diversity among the groups could help in understanding the evolutionary path of TNOs and/or the effects of different physical processes on their surfaces.

Each group contains objects whose spectra indicate particular compositional characteristics of the surface. The available spectra of members of each group are inside the error bars of the average broadband reflectance spectrum.

As a reference, we superposed on the average spectrum of each group a surface composition model obtained by interpreting the spectral characteristics of the group member for which the best quality spectrum was available (Fig. 2).

The *RR* group contains the reddest objects of the solar system. Spectra are available for 5145 Pholus (Cruikshank et al. 1998), 47171 1999 TC_{36} (Dotto et al. 2003a), 55576 2002 GB_{10} (Doressoundiram et al. 2005a), 83982 2002 GO_9 (Doressoundiram et al. 2003), and 90377 Sedna (Barucci et al. 2005). All surface composition models of these objects contain a few percent of H_2O ice on the surface. In Figure 2 the model of 1999 TC_{36} (Dotto et al. 2003a) has been superposed as a reference for the broadband reflectance of the group. The model is composed of 57% Titan tholin, 25% ice tholin, 10% amorphous carbon, and 8% water ice. The redness of the group could imply large amounts

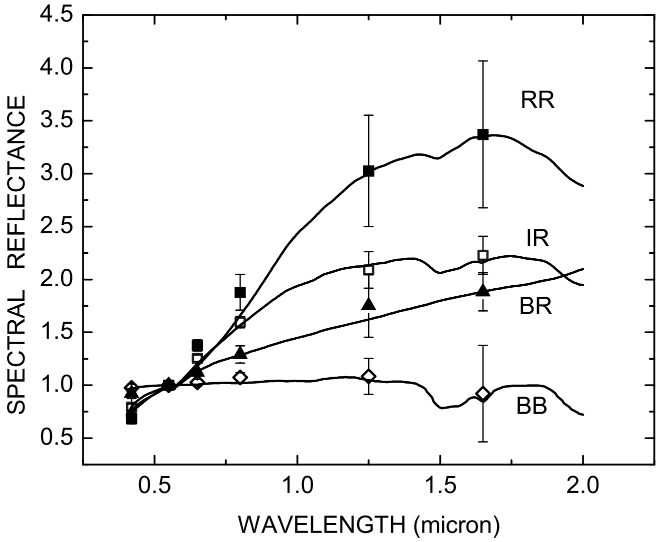

Fig. 3.—Four obtained groups reported with the average broadband reflectance spectra normalized to the *V* band (550 nm) and the relative error bars. For each group the compositional model of the spectrum of one of the members of the group is superposed. For *RR* the spectral model of 47171 1999 TC_{36} (Dotto et al. 2003a) is superposed; for *BB* the spectra of 90482 Orcus (Fornasier et al. 2004); for *IR* the spectra of 26375 1999 DE_9 (Doressoundiram et al. 2003); and for *BR* the spectra of 63252 2001 BL_{41} (Doressoundiram et al. 2005a).

of Titan tholin and/or ice tholin on the surface. Tholins are complex organic solids (Roush & Cruikshank 2004) produced by the irradiation of mixtures of cosmically abundant reducing gases and ices.

The *BB* group contains objects with a neutral reflectance spectra. Typical objects of the group with available spectra are 2060 Chiron (Luu et al. 2000; Romon-Martin et al. 2003), 90482 Orcus (Fornasier et al. 2004), 19308 1996 TO_{66} (Brown et al. 1999), and 15874 1996 TL_{66} (Luu & Jewitt 1998). The typical spectra are flat and somewhat bluish in the near-IR. The H_2O absorption bands seem generally stronger than in the other groups, although the H_2O ice presence in the Chiron spectrum seems connected to temporal/orbital variations, and the spectrum of 1996 TL_{66} is completely flat. The model spectrum of 90482 Orcus (Fornasier et al. 2004) has been associated with this class and is reported in Figure 2. It contains 4% Titan tholin, 85% amorphous carbon, and 11% water ice. The presence of large amounts of amorphous carbon (Zubko et al. 1996) is common to the members of this group.

The *IR* group is less red than *RR* group. Typical members of this group are 20000 Varuna (Licandro et al. 2001), 38628 Huya (de Bergh et al. 2004), 47932 2000 GN_{171} (de Bergh et al. 2004), 26375 1999 DE_9 (Jewitt et al. 2001; Doressoundiram et al. 2003), and 55565 2002 AW_{197} (Doressoundiram et al. 2005a). Three of these objects seem to contain hydrous silicates on the surface. The model spectrum reported in Figure 2 is that of the scattered object 26375 1999 DE_9 composed of 24% Titan tholin, 15% ice tholin, 54% amorphous carbon, and 7% water ice (Doressoundiram et al. 2003).

The *BR* group is an intermediate group between *BB* and *IR*, even if its color behavior is closer to that of the *IR* group. The typical members of this group are 8405 Asbolus (Barucci et al. 2000; Romon-Martin et al. 2002), 10199 Chariklo (Dotto et al. 2003b), 54598 Bienor (Dotto et al. 2003a), and 32532 Thereus (Barucci et al. 2002). A few percent of H_2O is present on the surface of these objects, but for Asbolus, Romon-Martin et al. (2002) did not find any ice absorption features during a complete rotational period. For this group we associated (Fig. 2) the surface composition model of Centaur 2001 BL_{41}, containing 17% Triton tholin, 10% ice tholin, and 73% amorphous carbon (Doressoundiram et al. 2005a).

The groups *BB* and *BR* have color spectra very similar to those of C-type and D-type asteroids. Unfortunately, we cannot associate an albedo range with each taxonomic group because of the lack of albedo data. The few available determinations based on ground observations are very uncertain: in fact, for the *RR* and *BB* groups, the albedo is known only for Pholus (0.04 ± 0.03; Davies et al. 1993) and Chiron (0.17 ± 0.02; Fernandez et al. 2002), respectively, while the albedo has been determined for two objects in both the *IR* and *BR* groups: Varuna (0.038 ± 0.022 by Lellouch et al. [2002]; 0.07 ± 0.03 by Jewitt et al. [2001]) and 55565 (0.17 ± 0.03 by Cruikshank et al. [2005]) in the *IR* group, and Asbolus (0.12 ± 0.03 by Fernandez et al. [2002]) and Chariklo (0.045 ± 0.010 by Jewitt & Kalas [1998]; 0.055 ± 0.008 by Altenhoff et al. [2001]) in the *BR* group.

Approximate fits to the characteristic spectra indicate that going from the neutral (*BB*) group to the very red (*RR*) group requires an increase in the content of organic material. The group *BB* in general does not require the presence of organic materials, as discussed by Cruikshank & Dalle Ore (2003). H_2O ice, even if not always detectable on the spectra, has to be present in all groups, as ices are expected to be a major constituent of this population.

We analyzed the behavior of each group with respect to the orbital elements and found an indication that almost all Centaurs are concentrated in the *BR* and *RR* groups (the *IR* group does not contain any Centaurs), confirming the Peixinho et al. (2003) result. In fact, Peixinho et al. reopened the TNO color controversy by arguing the existence of two color groups among the Centaurs and not in the TNO population. We found also that the average inclination of the orbits of the *RR* group members is the lowest, while that of the *BB* group members is the highest, mainly in the classical population. This is in agreement with previous results (Tegler & Romanishin 2000; Levison & Stern 2001; Brown 2001; Doressoundiram et al. 2002; Tegler et al. 2003). No relation between groups and TNO diameters has been found.

5. CONCLUSIONS

We have proposed a classification for TNOs and Centaurs based on their broadband colors using a two letter designation for each group (*BB*, *BR*, *IR*, and *RR*). Such a classification gives a snapshot on the similarities and/or differences among the objects.

We applied a multivariate statistical method (*G*-mode analysis) to a sample of 51 TNOs and Centaurs for which a homogeneous set of four colors ($B - V$, $V - R$, $V - I$, and $V - J$) are available. The results, obtained using a robust statistical analysis, show that the population is divided into four well-defined groups, confirming the preliminary results obtained by Barucci et al. (2001), who analyzed only 22 objects described by the same variables.

Analyzing a subsample of 37 objects for which a fifth variable (the $V - H$ color) was available yielded the same four groups, thus confirming the results. Using the extended version of the *G*-mode analysis for those objects with only three variable colors ($B - V$, $V - R$, and $V - I$), we obtained a preliminary classification for 84 other objects. Among these, 15 objects remain unclassified and 13 are assigned to two groups. The availability of the fourth variable ($V - J$) is indispensable for good statistical applications.

A model spectrum of one of the members has been associated to each group. The models that fit the reflectance spectra can be matched with synthetic spectra calculated with different percentages of ices, organics, and minerals. A higher content of organic material is necessary to fit the redder spectra, while only a small amount of H_2O ice is, in general, needed in all spectra. In fact, H_2O ice, which is supposed to be the bulk constituent of these bodies, could be hidden by low-albedo, opaque surface materials and for this reason may appear on the surface only in sparse outcrops.

Cruikshank & Dalle Ore (2003) modeled the full range of the redness of TNO and Centaur reflectance spectra with combinations of different percentages of organics and amorphous carbon without requiring the addition of space-weathered, igneous rock–forming minerals. However, Moroz et al. (2004) showed that space weathering is an important phenomenon that can influence the surface composition of these objects, and it is not well understood. In general, simulations of aging effects by ion irradiation show an increase in reddening. But some experiments on particularly dark material with red spectra (i.e., asphaltite) exhibit the opposite behavior: flattening of the spectra. The direction of the trend is difficult to interpret without knowledge of the albedos. Albedo is an important parameter for the analysis of surface composition, and the knowledge of it for a large number of objects, which will increase with *Spitzer* observations, will be fundamental for the statistical analysis of the TNO population.

We can conclude that multivariate statistical analysis of broad bands of visible and near-IR colors provides a strong indication for differences in the surface natures of the TNO population. The obtained different groups indicate the present physico-chemical surface state of the analyzed objects. The trend from neutral (*BB*) to very red (*RR*) groups indicates the possible sequence of alteration processes (collisions, resurfacing, craters, UV and/or energetic particle bombardment, etc.). Each group would represent an evolutionary stage of the population, indicating the duration for which each object has been exposed to these different alteration processes. The relative number of objects in each group would account for the time spent in the different evolutionary stages. The presence of a single-object group could imply the possible existence of another class. As more objects are discovered and more data are available on their properties, our classification scheme may have to be expanded by the addition of more groups. Clearly, more observations at different wavelengths and laboratory work will be indispensable to enhancing our understanding of the different classes and evolutions of the TNO population.

REFERENCES

Altenhoff, W. J., Menten, K. M., & Bertoldi, F. 2001, A&A, 366, L9

Barucci, M. A., Capria, M. T., Coradini, A., & Fulchignoni, M. 1987, Icarus, 72, 304

Barucci, M. A., Cruikshank, D. P., Dotto, E., Merlin, F., Poulet, F., Dalle Ore, C., Fornasier, S., & de Bergh, C. 2005, A&A, in press

Barucci, M. A., de Bergh, C., Cuby, J.-G., Le Bras, A., Schmitt, B., & Romon, J. 2000, A&A, 357, L53

Barucci, M. A., Doressoundiram, A., & Cruikshank, D. 2004, in Comets II, ed. M. Festou et al. (Tucson: Univ. Arizona Press), 647

Barucci, M. A., Doressoundiram, A., Tholen, D., Fulchignoni, M., & Lazzarin, M. 1999, Icarus, 142, 476

Barucci M. A., Fulchignoni, M., Birlan, M., Doressoundiram, A., Romon, J., & Boehnhardt, H. 2001, A&A, 371, 1150

Barucci, M. A., et al. 2002, A&A, 392, 335

Bauer, J. M., Meech, K. J., Fernández, Y. R., Pittichova, J., Hainaut, O. R., Boehnhardt, H., & Delsanti A. C. 2003, Icarus, 166, 195

Binzel, R. P., & Xu, S. 1993, Science, 260, 186

Boehnhardt, H., et al. 2001, A&A, 378, 653

———. 2002, A&A, 395, 297

Brown, M. E. 2001, AJ, 121, 2804

Brown, R. H., Cruikshank, D. P., & Pendleton, Y. 1999, ApJ, 519, L101

Bus, S. J., & Binzel, R. P. 2002, Icarus, 158, 146

Coradini, A., Fulchignoni, M., Fanucci, O., & Gavrishin, A. I. 1977, Comput. Geosci., 3, 85

Cruikshank, D. P., & Dalle Ore, C. 2003, Earth Moon Planets, 92, 315

Cruikshank, D. P., Stansberry, J. A., Emery, J. P., Fernandez, Y. R., Werner, M. W., Trilling, D. E., & Rieke, G. H. 2005, ApJ, 624, L53

Cruikshank, D. P., et al. 1998, Icarus, 135, 389

Davies, J. K. 2000, in Minor Bodies in the Outer Solar System, ed. A. Fitzsimmons et al. (Berlin: Springer), 9

Davies, J. K., Green, S., McBride, N., Muzzerall, E., Tholen, D. J., Whiteley, R. J., Foster, M. J., & Hillier, J. K. 2000, Icarus, 146, 253

Davies, J. K., McBride, N., Ellison, S. L., Green, S. F., & Ballantyne, D. R. 1998, Icarus, 134, 213

Davies, J. K., McBride, N., & Green, S. F. 1997, Icarus, 125, 61

Davies, J. K., Spencer, J., Sykes, M., Tholen, D., & Green S. 1993, IAU Circ. 5698

Davies, J. K., et al. 2001, Icarus, 150, 69

de Bergh, C., Delsanti, A., Tozzi, G. P., Dotto, E., Doressoundiram, A., & Barucci, M. A. 2005, A&A, 437, 1115

de Bergh, C., et al. 2004, A&A, 416, 791

Delsanti, A., Hainaut, O., Jourdeuil, E., Meech, K., Boehnhardt, H., & Barrera L. 2004, A&A, 417, 1145

Delsanti, A., Peixinho, N., Merlin, F., Davies, J. K., Doressoundiram, A., Boehnhardt, H., & Barucci, M. A. 2005, Icarus, submitted

Delsanti, A. C., Boehnhardt, H., Barrera, L., Meech, K. J., Sekiguchi, T., & Hainaut, O. R. 2001, A&A, 380, 347

Doressoundiram, A. 2003, Earth Moon Planets, 92, 131

Doressoundiram, A., Barucci, M. A., Boehnhardt, H., Tozzi, G. P., Poulet, F., de Bergh, C., & Peixinho, N. 2005a, Planet. Space Sci., in press

Doressoundiram, A., Barucci, M. A., Romon, J., & Veillet, C. 2001, Icarus, 154, 277

Doressoundiram, A., Peixinho, N., de Bergh, C., Fornasier, S., Thébault, P., Barucci, M.A., & Veillet, C. 2002, AJ, 124, 2279

Doressoundiram, A., Peixinho, N., Doucet, C., Mousis, O., Barucci, M. A., Petit, J. M., & Veillet, C. 2005b, Icarus, 174, 90

Doressoundiram, A., Tozzi, G. P., Barucci, M. A., Boehnhardt, H., Fornasier, S., & Romon, J. 2003, AJ, 125, 2721

Dotto, E., Barucci, M. A., Boehnhardt, H., Romon, J., Doressoundiram, A., Peixinho, N., de Bergh, C., & Lazzarin, M. 2003a, Icarus, 162, 408

Dotto, E., Barucci, M. A., Leyrat, C., Romon, J., de Bergh, C., & Licandro, J. M. 2003b, Icarus, 164, 122

Farnham, T. L., & Davies, J. K. 2003, Icarus, 164, 418

Fernandez, Y. R., Jewitt, D. C., & Sheppard, S. S. 2002, AJ, 123, 1050

Ferrin, I., et al. 2001, ApJ, 548, L243

Fornasier, S., Dotto, E., Barucci, M. A., & Barbieri, C. 2004, A&A, 422, L43

Fulchignoni, M., Birlan, M., & Barucci, M. A. 2000, Icarus, 146, 204

Fulchignoni, M., Delsanti, A., Barucci, M. A., & Birlan, M. 2003, Earth Moon Planets, 92, 243

Gil-Hutton, R., & Licandro, J. 2001, Icarus, 152, 246

Hainaut, O. R., et al. 2000, A&A, 356, 1076

Hardorp, J. 1980, A&A, 91, 221

Hartmann, W. K., Cruikshank, D. P., & Degewij, J. 1982, Icarus, 52, 377

Jewitt, D. C., Aussel, H., & Evans, A. 2001, Nature, 411, 446

Jewitt, D. C., & Kalas, P. 1998, ApJ, 499, L103

Jewitt, D. C., & Luu, J. X. 1998, AJ, 115, 1667

———. 2001, AJ, 122, 2099

Lellouch, E., Moreno, R., Ortiz, J. L., Paubert, G., Doressoundiram, A., & Peixinho, N. 2002, A&A, 391, 1133

Levison, H. F., & Stern, S. A. 2001, AJ, 121, 1730

Licandro, J., Oliva, E., & Di Martino, M. 2001, A&A, 373, L29

Luu, J. X., & Jewitt, D. C. 1996, AJ, 112, 2310

———. 1998, ApJ, 494, L117

Luu, J. X., Jewitt, D. C., & Trujillo, C. 2000, ApJ, 531, L151

McBride, N., Davies, J. K., Green, S. F., & Foster, M. J. 1999, MNRAS, 306, 799

McBride, N., Green, S. F., Davies, J. K., Tholen, D. J., Sheppard, S. S., Whiteley, R. J., & Hillier, J. K. 2003, Icarus, 161, 501

Moroz, L., Baratta, G., Strazzulla, G., Starukhina, L., Dotto, E., Barucci, M. A., Arnold, G., & Distefano, E. 2004, Icarus, 170, 214

Peixinho, N., Boehnhardt, H., Belskaya, I., Doressoundiram, A., Barucci, M. A., & Delsanti, A. 2004, Icarus, 170, 153

Peixinho, N., Doressoundiram, A., Delsanti, A., Boehnhardt, H., Barucci, M. A., & Belskaya, I. 2003, A&A, 410, L29

Romanishin, W., Tegler, S. C., Levine, J., & Butler, N. 1997, AJ, 113, 1893

Romon-Martin, J., Barucci, M. A., de Bergh, C., Doressoundiram, A., Peixinho, N., & Poulet, F. 2002, Icarus, 160, 59
Romon-Martin, J., Delahodde, C., Barucci, M. A., de Bergh, C., & Peixinho, N. 2003, A&A, 400, 369
Roush, T. L., & Cruikshank, D. P. 2004, in Astrobiology: Future Perspectives, ed. P. Ehrenfreund (Dordrecht: Kluwer), 149
Schaefer, B. E., & Rabinowitz, D. L. 2002, Icarus, 160, 52
Sheppard, S. S., & Jewitt, D. C. 2002, AJ, 124, 1757
Tegler, S. C., & Romanishin, W. 1997, Icarus, 126, 212
———. 1998, Nature, 392, 49
Tegler, S. C., & Romanishin, W. 2000, Nature, 407, 979
———. 2003, Icarus, 161, 181
Tegler, S. C., Romanishin, W., & Consolmagno, S. J. 2003, ApJ, 599, L49
Tholen, D. J. 1984, Ph.D. thesis, Univ. Arizona, Tucson
Tholen, D. J., & Barucci, M. A. 1989, in Asteroids II, ed. R. P. Binzel & T. Gehrels (Tucson: Univ. Arizona Press), 298
Trujillo, C. A., & Brown, M. E. 2002, ApJ, 566, L125
Zubko, V. G., Mennella, V., Colangeli, L., & Bussoletti, E. 1996, MNRAS, 282, 1321